



Simulated Investigation on the Impact of Spatial–temporal Variability of Rainstorms on Flash Flood Discharge Process in Small Watershed

Guangzhao Chen¹ · Jingming Hou¹  · Yuan Hu¹ · Tian Wang¹ · Shaoxiong Yang¹ · Xujun Gao²

Received: 28 September 2022 / Accepted: 25 November 2022 / Published online: 19 January 2023
© The Author(s), under exclusive licence to Springer Nature B.V. 2023

Abstract

With the spatial–temporal variability of rainstorms becoming more diversified, it is urgent to summarize how the spatial–temporal variability of rainstorm affects the flash flood discharge process and to explore its internal mechanism. This work proposes a research framework based on the rainstorm spatial–temporal structure design method and the quantitative analysis of flash flood discharge process modeling. This framework generates rainstorm data with different spatial–temporal variability through the rainstorm spatial–temporal structure design method, and further simulates discharge process under different rainstorm scenarios through the hydrodynamic model. Based on the analysis of simulated results, the error correction coefficient is generated to improve the accuracy of simulation. In this study, the Baogaisi watershed was used for simulation. The results show that when the rainstorm center is at the upstream watershed, the peak discharge increases, and the flood peak time is advanced because of the transformation of gravitational potential energy into kinetic energy. When the rainstorm center is fixed at a position, the total flood volume and the peak discharge are about 2~10 times that of uniform spatial distributed scenario, the flood peak time can be advanced to 55 min. In the mobile rainstorm, the peak discharge and the total flood volume are significantly reduced and the flood peak time is lagged, the flood peak discharge can be reduced by up to 30% of the uniform spatial distributed scenario. Strengthening the understanding of the impact can help to improve the accuracy of discharge process simulation.

Keywords Flash flood · Spatial–temporal variability · Rainstorm · Discharge process · Numerical simulation

✉ Jingming Hou
jingming.hou@xaut.edu.cn

¹ State Key Laboratory of Eco-Hydraulics in Northwest Arid Region, Xi'an University of Technology, Xi'an 710048, Shaanxi, China

² China Power Construction Group, Co. LTD, Northwest Eng. Corp. Ltd., Xi'an 710065, Shaanxi, China

1 Introduction

A flash flood is commonly triggered by heavy and intense rainstorm and occurs in mountainous catchments of a few hundred square kilometers (Ahmadalipour and Moradkhani 2019). A flash flood disaster is highly destructive and brings heavy losses due to secondary disasters, such as landslides and debris flows (Karbasi et al. 2018). As extreme rainstorm become more frequent, it is predicted that the potential damage of flash flood worldwide is expected to reach 1 trillion US dollars by 2050 (Bubeck and Thielen 2018).

Rainstorm is a heterogeneous process in space and time over a wide range of scales (Zoccatelli et al. 2011). The effect of spatial–temporal heterogeneity of rainstorm on flash flood discharge process is a question that has been frequently explored in hydrology. Yuan et al. (2021) proposed three characteristic parameters to describe the temporal distribution characteristics of rainfall processes, and using the hydrological model to simulate the rainfall–runoff process under the condition of artificial rainfall process. Yuan et al. (2022) proposed a random rainfall pattern generation method for simulating flash flood, which can generate rainstorm data with comprehensive rain peak position coefficient. Saharia et al. (2021) adopted a big-sample method to do a quantification of the effects of spatial variability of rainstorm on flash flood. For more effective watershed monitoring and modeling, the response of rainstorm spatial–temporal variability to watershed flooding has also been investigated. Zoccatelli et al. (2010) found that ignoring the spatial variability of rainstorm leads to a significant decrease of modeling performance in small watersheds (36–167 km²). Zoccatelli et al. (2011) explored the effects of space–time aggregation on flood modeling, and developed the stochastic storm transposition (SST), which is a physically based stochastic rainfall generator. Yang et al. (2016) concluded that the impact of rainstorm spatial variability is strongly linked to the peak rain rate and weakly linked to soil moisture conditions.

Most of the conclusions on the effects of spatial–temporal heterogeneity of rainstorm on flash flood discharge process are based on a relatively limited number of watersheds and rainstorm events. Tarolli et al. (2012) summarized the relationship between 13 flash flood events and climatic variability in Mediterranean area and found a peculiar seasonality impact on flash flood. Llasat et al. (2014) analyzed flash flood events that affected Catalonia, clarifying that flash flood occurs as a result of highly convective rainstorm which is short, localized, and intense. Silvestro et al. (2016) investigated how the temporal-spatial pattern of rainstorm exerted an impact on the runoff generation and evolution based on flash flood monitoring data. Since flash floods are the product of complex interactions between rainfall and terrain characteristics, the above conclusions drawn from specific watersheds and specific rainstorm events may be somewhat specific (Wright et al. 2014). The existing literatures have not yielded a consensus, which implies a need for further understanding of flash flood discharge process (Saharia et al. 2021).

Many researches have been conducted to analyze regional rainstorm processes caused by different weather systems in terms of water vapor condition, dynamic and thermodynamic mechanisms (Yu et al. 2015; Zhang et al. 2017; Li et al. 2018a; Ding et al. 2018; Hu et al. 2021). These researches summarized the development and evolution of rainstorm system, and stated that the arising, shift, and disappearance of rainstorms can be broadly classified into two types, i.e., stationary and mobile. The stationary rainstorm refers to the fact that in a rainstorm event, the spatial distribution of rainstorm is basically unchanged, while the mobile rainstorm refers to that in a rainstorm event, the spatial distribution of rainstorm varies significantly with

time. Although considerable progress of rainfall monitoring has been made, long-term high-resolution monitoring data are still lacking (Lopez-cantu and Samaras 2018).

This work proposed a research framework based on the rainstorm spatial-temporal structure design method and the quantitative analysis of flash flood modeling. This framework can generate a large amount of high-resolution rainstorm data with different spatial-temporal variability, which can solve the problem of insufficient data of high-resolution rainstorm. Further, the impact of spatial-temporal variability of rainstorms on discharge process were derived by simulating hydrographs with a hydrodynamic model. Lastly, this work constructed an error correction coefficient matrix based on the result analysis, which can improve the accuracy of simulation in the study area.

2 Methods and Data

2.1 2D Hydrodynamic Model

The GAST (GPU Accelerated Surface Water Flow and Associated Transport) model is coupled with hydrological and hydrodynamic processes (Hou et al. 2021). In a flood event, the magnitude of water depth is generally much smaller than the horizontal inundation extent, and the flow hydrodynamics can be mathematically described by the shallow water equations (SWEs). The SWEs can be written as:

$$\frac{\partial q}{\partial t} + \frac{\partial f}{\partial x} + \frac{\partial g}{\partial y} = S \tag{1}$$

$$\begin{aligned}
 \mathbf{q} &= \begin{bmatrix} h \\ q_x \\ q_y \end{bmatrix}, \quad \mathbf{f} = \begin{bmatrix} uh \\ uq_x + gh^2/2 \\ uq_y \end{bmatrix}, \quad \mathbf{g} = \begin{bmatrix} vh \\ vq_x \\ vq_y + gh^2/2 \end{bmatrix} \\
 \mathbf{S} &= \begin{bmatrix} i \\ -\frac{gh\partial z_b}{\partial x} - C_f u \sqrt{u^2 + v^2} \\ -\frac{gh\partial z_b}{\partial y} - C_f v \sqrt{u^2 + v^2} \end{bmatrix}
 \end{aligned} \tag{2}$$

where t denotes the time; x and y represent the Cartesian coordinates; \mathbf{q} is the vector of flow variables containing the water depth h , in which q_x and q_y are discharges in the x - and y - directions, respectively; u and v are depth-averaged velocities in the x - and y - directions, respectively; z_b denotes the bed elevation; \mathbf{f} and \mathbf{g} are the flux vectors in the x - and y - directions, respectively; \mathbf{S} represents the source vector; i equals to $i_r - i_i$, where i_r is the rainfall rate while i_i denotes the infiltration rate. C_f is the bed roughness coefficient.

Infiltration rate is another parameter that influence the simulated performance, especially when the watershed under consideration is dry. In GAST, the Green-Ampt (G-A) model is used to describe the soil infiltration characteristics (Hou et al. 2021). The equation is as follows:

$$f_p = \begin{cases} P \\ K_S [1 + (\theta_s - \theta_i) S_f / I_p] \end{cases} \tag{3}$$

where f_p is the soil infiltration rate, (mm/min); K_S is the soil saturated hydraulic conductivity, (mm/min); θ_i is the initial soil water content; θ_S is the saturated soil water content; S_f is the wetting front suction, (mm); P is the rainfall intensity, (mm/min); I_p is the accumulated infiltration, (mm).

2.2 Data

2.2.1 Watershed Data

Baogaisi watershed is at Hunan Province, China, with a total area of 56 km². The information of location and terrain is shown in Fig. 1. The river channel is about 20 km long and has an average slope of about 4%. Its bank sides are steep and the slope is about 4.5%. The watershed is in a humid subtropical climate zone with the average annual precipitation about 1569 mm. The Qingshui hydrological station has been set up in the downstream. The precipitation data and water depth data for model validation are obtained from the hydrological station. The average discharge recorded by the hydrological station is 0.75m³/s. The watershed is prone to flash flood disasters in summer. On June 3, 2020, the cumulative rainfall monitored by the hydrological station reached 195 mm, the area of flooded farmland in the lower reaches of the watershed exceeded 100 hectares and the local traffic was temporarily interrupted.

2.2.2 Rainstorm Data Generation

This work used the rainstorm design method to generate large amounts of high-resolution spatial–temporal structure data for rainstorm. The rainstorm design method is composed of the Chicago rain pattern and the Krigin interpolation method. Data for the two typical rainstorm scenarios described above are generated to serve as input data for the GAST model.

Rainstorm Temporal Distribution The Chicago rain pattern is a non-uniform design rain pattern proposed by Keifer and Chu (1957). The Chicago rain pattern designs a typical

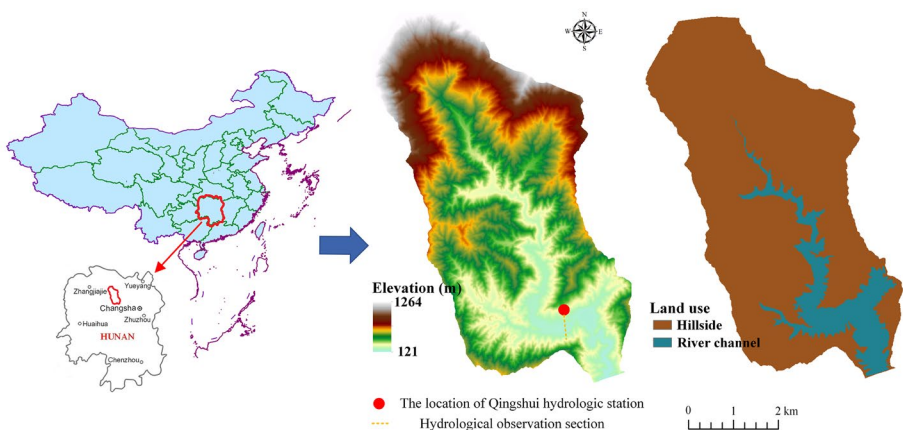


Fig. 1 The location and terrain data of the Baogaisi watershed

rainfall process based on the statistical rainfall intensity formula. The rainfall time series is divided into two parts, pre-peak and post-peak, by introducing the rain peak coefficient r to describe the moment when the rainstorm peak occurs (Li et al. 2018b). The equation for the rainstorm intensity in the study area is Eqs. (4)–(6). The parameters used in these equations were derived by experts organized by the local government.

$$i = \frac{A(1 + C \lg P)}{(t + b)^n} = \frac{1141.9(1 + 0.54 \lg P)}{(t + 8.277)^{0.5127}} \tag{4}$$

where i is the rainfall intensity (mm/min), P is the return period (a), and t is the rainfall duration (min), n is the rainfall attenuation index, A , b and C are the constant.

$$i_a = \frac{a \left[\frac{(1-n)t_a}{r} + b \right]}{\left(\frac{t_a}{r} + b \right)^{1+c}} \tag{5}$$

$$i_b = \frac{a \left[\frac{(1-n)t_b}{1-r} + b \right]}{\left(\frac{t_b}{1-r} + b \right)^{1+c}} \tag{6}$$

where t_a is the pre-peak rainfall duration (min), t_b is the post-peak rainfall duration, (min), a is a constant equaling to $A(1 + C \lg P)$; n and b together reflect the design rainfall intensity decreasing with the extension of the duration, and their parameters take the same values as those in Eq. 4.

Ochoa-Rodriguez et al. (2015) investigated the rainstorm temporal-resolution requirements for hydrodynamic modelling based on multiple rainfall-flooding data, and identified the optimal temporal-resolution applicable to the simulation as 5 min. And the Chicago rain pattern is only suitable for generating the rainfall process with short-duration (Li et al. 2018b). Therefore, the rainstorm temporal-resolution is 5 min, and the duration is 2 h in this work. Three rainstorm types derived from the Chicago rain pattern (rain peak coefficient $r=0.2, 0.5, 0.8$) were designed. Percentage distribution of these three rainstorm types is shown in Fig. 2. As r increases, the location of the rain peak gradually shifts backward. The three rain types correspond to the situation that the time of peak rainfall intensity is at the beginning, middle and end of a rainstorm event. Based on the principle of small to large and equal rainfall interval, five accumulative rainfall amounts (20, 40, 60, 80, 100 mm) were selected to study the impact of rainfall amount variation.

Rainstorm Spatial Distribution The study area involved in this work is small (56 km²). Therefore, only spatially single-peaked pattern of rainstorm was considered for this watershed in this work. The watershed area division is provided in Fig. 3 (yellow line). According to the reference (Notaro et al. 2013; Gires et al. 2014; Ochoa-Rodriguez et al. 2015), the spatial resolution of rainfall cell is set to 500 m. Therefore, the entire watershed is divided into 234 rainfall cells. In addition, the entire watershed is divided into three parts along the river direction, i.e., upstream watershed, midstream watershed, and downstream watershed, as shown in Fig. 3.

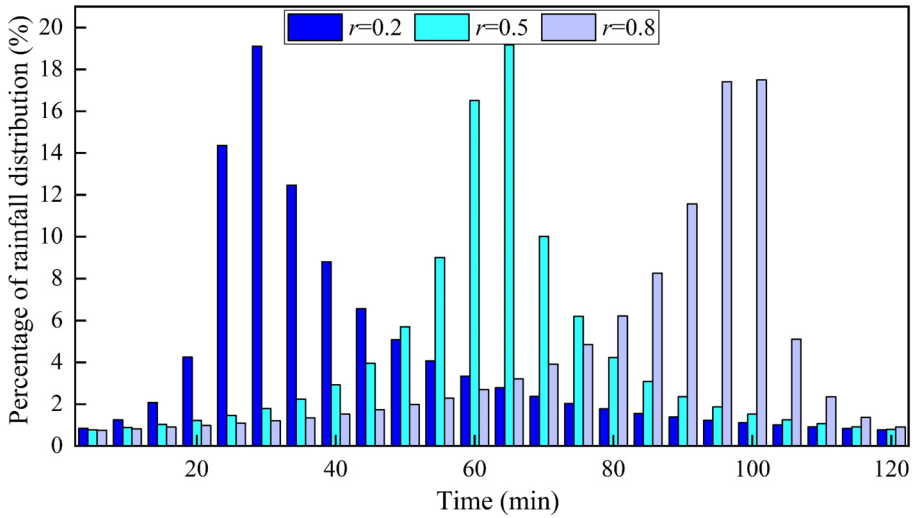


Fig. 2 Percentage distribution of three rainstorm types

The first simulated scenario is that the rainstorm center is at a position in the watershed and will not change in a rainstorm event. In this work, the rainstorm centers are designed to be located at upstream watershed, midstream watershed, and downstream watershed, respectively. The second simulated scenario is that the rainfall field moves along a direction, that is to say, the area where it is raining gradually expands in one direction. Based on

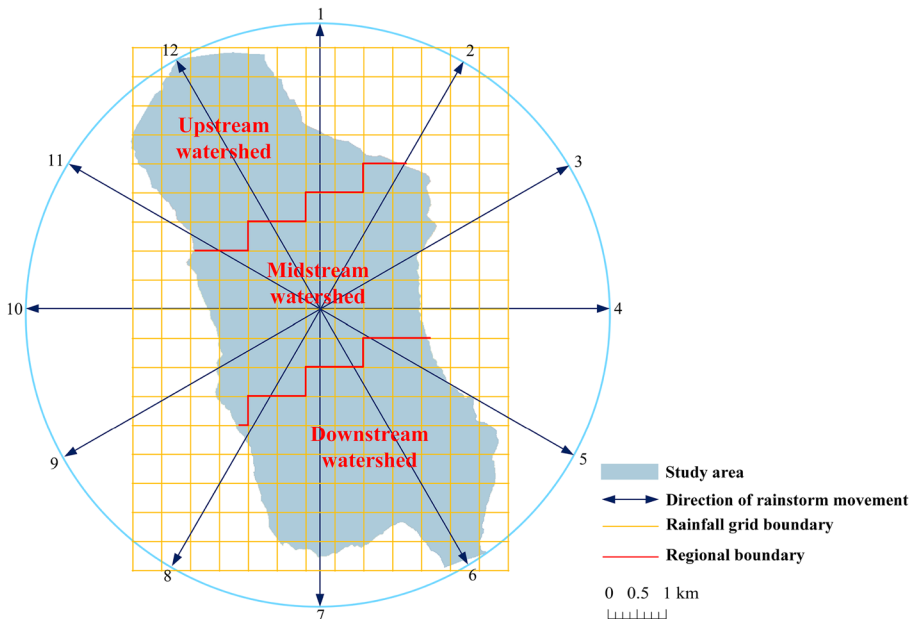


Fig. 3 Rainstorm spatial distribution of the Baogaisi watershed

the research conclusion of Liang (2010) about the move speed of rainfall field in the watershed, this work sets the speed as 1.0 km/h (500 m/5 min). Twelve directions are divided, with 30° intervals between two directions, as shown in Fig. 3. These moving directions cover all angles in which rainstorm can move over the watershed, so the changes of flash flood discharge caused by rainstorms with different moving paths can be systematically simulated.

The rainfall data of each rainfall cell are obtained by Krigin interpolation method in the ArcGIS software to obtain the rainfall data with a spatial resolution of 500 m. In ArcGIS software, control points are set up uniformly every 1 km along the northwest-southeast direction of the river channel. In each rainstorm scenario, the rainfall amount at the control point where the rainstorm center is located is the maximum; the rainfall amount at other control points gradually decreases as the distance from the control point at the rainstorm center increases. Figure 4a demonstrates the rainfall distribution of the stationary scenario with 20 mm accumulative rainfall. Figure 4b shows the rainfall distribution with the 60 mm accumulative rainfall and No. 6 moving direction.

In the stationary rainstorm scenario, there are 4 types of the rainstorm center, 3 types of the rain peak coefficient, and 5 types of the accumulative rainfall. The total number of simulated cases is $4 \times 3 \times 5 = 60$. In the mobile rainstorm scenario, there are 12 types of the moving direction, 3 types of the rain peak coefficient, and 5 types of the accumulative rainfall. The total number of simulated cases in this scenario is $12 \times 3 \times 5 = 180$. The rainstorm process of each rainfall cell is consistent. In this work, mobile rainstorm simulation was implemented through controlling the starting and ending time of the rainstorm process in each rainfall cell to realize rainstorm movement. Variables and value range of rainstorm scenarios are listed in Table 1.

2.3 Evaluation Indicator

To evaluate the simulated performance of the hydrodynamic model, the simulation results are compared with the measured data, and the Nash–Sutcliffe efficiency (NSE) is used to evaluate the simulated performance. The formula is Eq. (7). If NSE is on the brink of 1, it means the simulated result is perfect.

$$NSE = 1 - \frac{\sum_{i=1}^n (q_o^i - q_p^i)^2}{\sum_{i=1}^n (q_o^i - \bar{q}_o)^2} \tag{7}$$

where q_o^i is the simulated data at time i ; q_p^i is the measured data at time i ; \bar{q} is the average of measured data.

The root mean square error (RMSE) is another common index for assessing model performance. $RMSE=0$ means that the simulated data matches the measured data exactly; if the RMSE is less than half of the standard deviation (σ) of the measured data, the model has good performance. The formula is as follows:

$$RMSE = \sqrt{\frac{\sum_{i=1}^n (Q_m^i - Q_s^i)^2}{n}} \tag{8}$$

where Q_m^i is the measured data at time i ; Q_s^i is the simulated data at time i ; n is the amount of data.

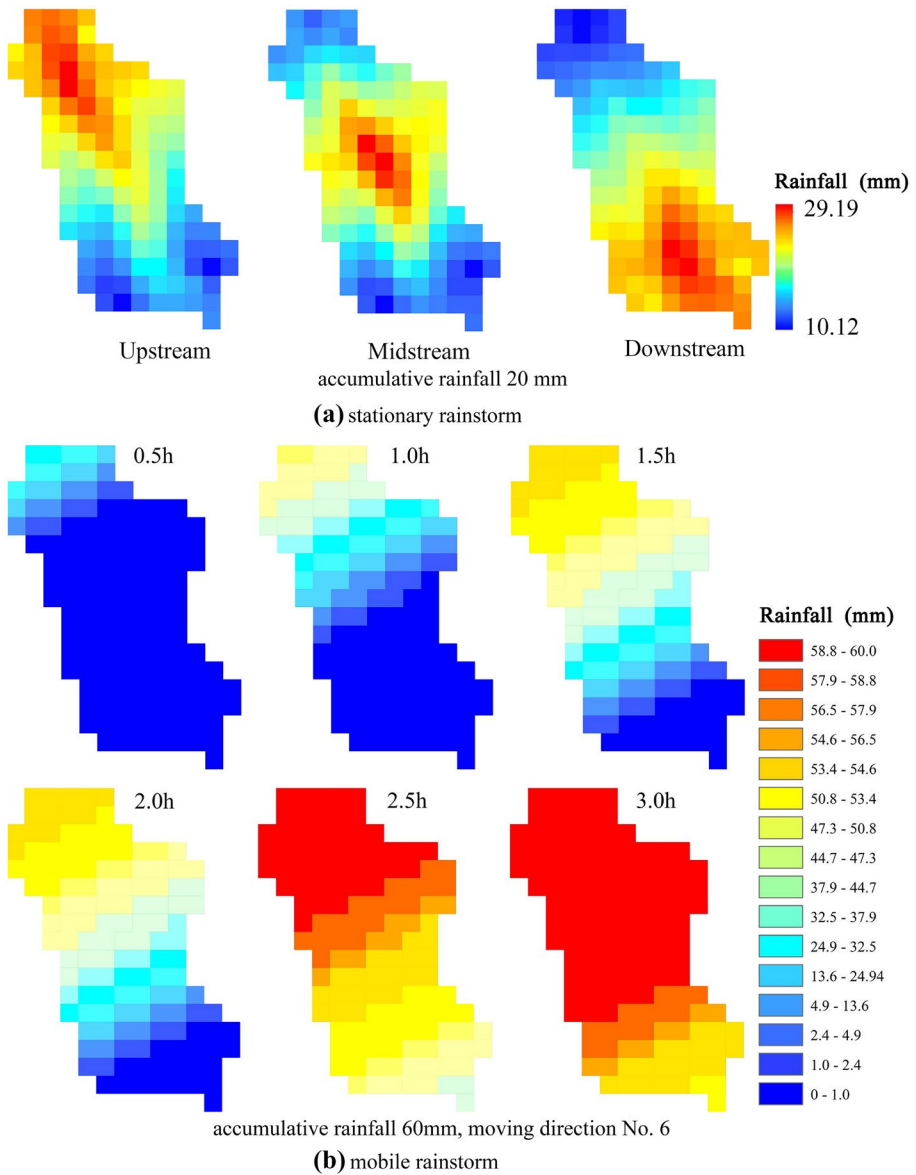


Fig. 4 The rasterized rainstorm distribution

The mean absolute percentage error (MAPE) is an index to evaluate the accuracy of numerical model. The smaller the MAPE, the higher the simulation accuracy of the numerical model. The formula is as follows:

Table 1 Variables and value range of rainstorm scenarios

Rainstorm scenario	Rainstorm variable	Rainstorm center	Rain peak coefficient	Accumulative rainfall	
Stationary rainstorm	Variable value	x_1	Upstream watershed	0.2	20
		x_2	Midstream watershed	0.5	40
		x_3	Downstream watershed	0.8	60
		x_4	Uniformly distributed	/	80
		x_5	/	/	100
Mobile rainstorm	Variable value		No. moving direction	Rain peak coefficient	Accumulative rainfall
		x_1	1	0.2	20
		x_2	2	0.5	40
		x_3	3	0.8	60
		x_4	4	/	80
		x_5	5	/	100
		x_6	6	/	/
		x_7	7	/	/
		x_8	8	/	/
		x_9	9	/	/
		x_{10}	10	/	/
		x_{11}	11	/	/
x_{12}	12	/	/		

$$MAPE = \frac{1}{n} \sum_{i=1}^n \left| \frac{Q_m^i - Q_s^i}{Q_m^i} \right| \tag{9}$$

where, the meaning of parameters is the same as that in Eq. (8).

The inequality degree I is used to make a quantitative evaluation of the impacts of the spatial and temporal variability of rainstorms, whose formula is Eq. (10). If the inequality degree I is greater than 1, it means that the impact of spatial and temporal variability of rainstorms makes the discharge increase, and vice versa.

$$I = \frac{Q_{DR}}{Q_R} \tag{10}$$

where Q_{DR} is the flash flood element corresponding to a rainstorm case with moving direction D and accumulative rainfall R ; Q_R is the flash flood element corresponding to the uniformly distributed rainstorm with accumulative rainfall R .

3 Model Validation

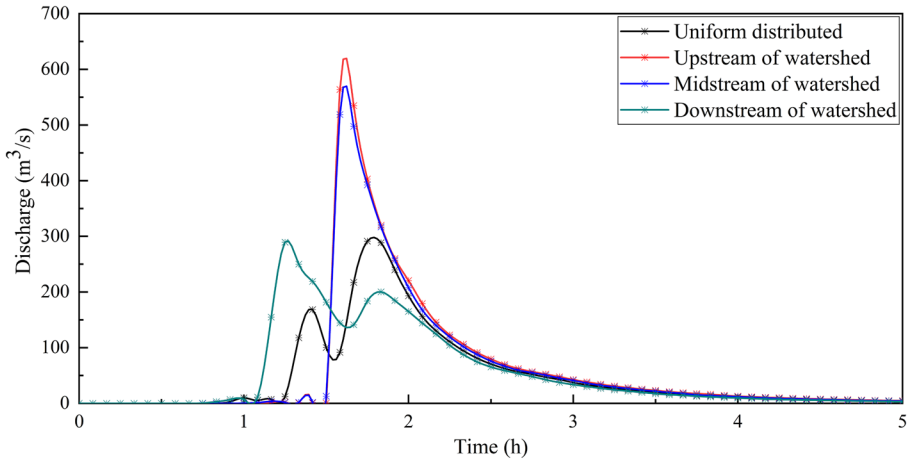
The precipitation data for the model validation is from May 9, 2012 (case 1), and June 6, 2013 (case 2). The NSE, RMSE, and MAPE value of the case 1 are 0.95, 0.048, 0.00023, relatively. However, these index values of case 2 are 0.92, 0.051, 0.00024, respectively. It illustrates that this model has high simulated accuracy for the watershed. More detailed validation information has been supplemented in the article attachment.

4 Results

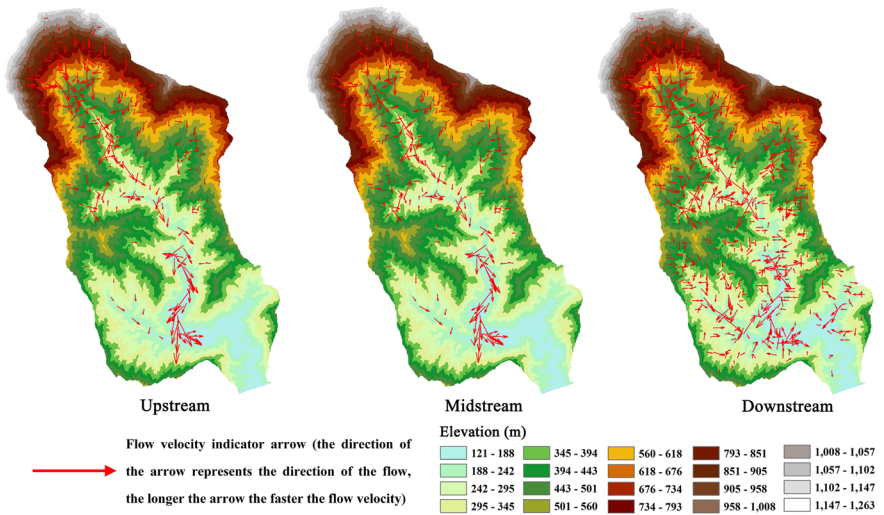
4.1 Impact of Stationary Rainstorm on Flash Flood Discharge Process

The simulation results of different stationary rainstorm scenario are similar. Due to the limited length of the article, the rainfall amount of 40 mm and the rain peak coefficient $r=0.5$ are taken as an example to show the simulation results of flash flood discharge process in Fig. 5. From Fig. 5a, the peak discharge under the conditions of different rainstorm centers reaches more than $300 \text{ m}^3/\text{s}$. The peak discharge is far greater than the average discharge of $0.75 \text{ m}^3/\text{s}$ recorded by Qingshui hydrological station. Therefore, the discharge process of uniform spatial distributed rainstorm at this time will lead to flooding risk. The discharge process of uniform spatial distributed rainstorm in Fig. 5a is a bimodal pattern. When the rainstorm center is at the upstream and midstream watershed, the discharge process turns into a single-peaked pattern. Therefore, the peak discharge increases significantly and the time for peak discharge is advanced at this situation, which increases flood risk. The flow velocity map at the flood peak time is shown in Fig. 5b. In the case of flat terrain, the peak flow is higher as the distance between the rainstorm center and the outlet of the basin decreases. When the rainstorm center is at the upstream and midstream watershed, the variation of the discharge process is different from the flow situation at the flat terrain. The flow velocity arrow in the river is very dense and long when the rainstorm center is at the upstream and midstream watershed, but the arrow is sporadic and short when the rainstorm center is at the downstream watershed. It shows that when the rainstorm center is at the upstream and midstream watershed, the runoff from the hillside converges to the river channel, with a high flow velocity.

Figure 6 illustrates the inequality degree of discharge characteristics. When the accumulative rainfall is 20 mm, the location of rainstorm center exerts the greatest influence on discharge characteristics; when the accumulative rainfall is 100 mm, the location of rainstorm center has the least influence. With the increase of accumulated rainfall, the inequality degree gradually decreases. The inequality degree of the flood peak discharge and the total flood volume is least when the rainstorm center is at the downstream watershed; whereas it is larger when the rainstorm center is at the upstream watershed. When the rainfall center is fixed at a position, the total flood volume and peak discharge are about 2~10 times that of uniform spatial distributed scenario, the flood peak time can be advanced to 55 min. The reduction of the flood peak time is the greatest when the rainstorm center is at the downstream watershed; whereas when rainstorm center is at the upstream and midstream watershed, the reduction is smaller than when it is at the downstream. From the data shown in Fig. (6), the discharge characteristics change little



(a) Hydrograph at the outlet of watershed



(b) Flow velocity map at the flood peak time

Fig. 5 Flash flood discharge process of outlet (40 mm, $r=0.5$)

under different rain peak coefficients. It proves that the impact of different rain peak coefficient r on discharge process is insignificant.

4.2 Impact of Mobile Rainstorm on Flash Flood Discharge Process

The response of discharge process to the rainstorm changes under different moving paths and different rainfall magnitudes is analyzed. The inequality degree of peak discharge is shown in Fig. 7 (a). The inequality degree of peak discharge under different moving directions is less than 1. This shows that under the condition of moving rainstorm, the peak discharge will decrease. Among them, the average of the inequality degree of each simulation

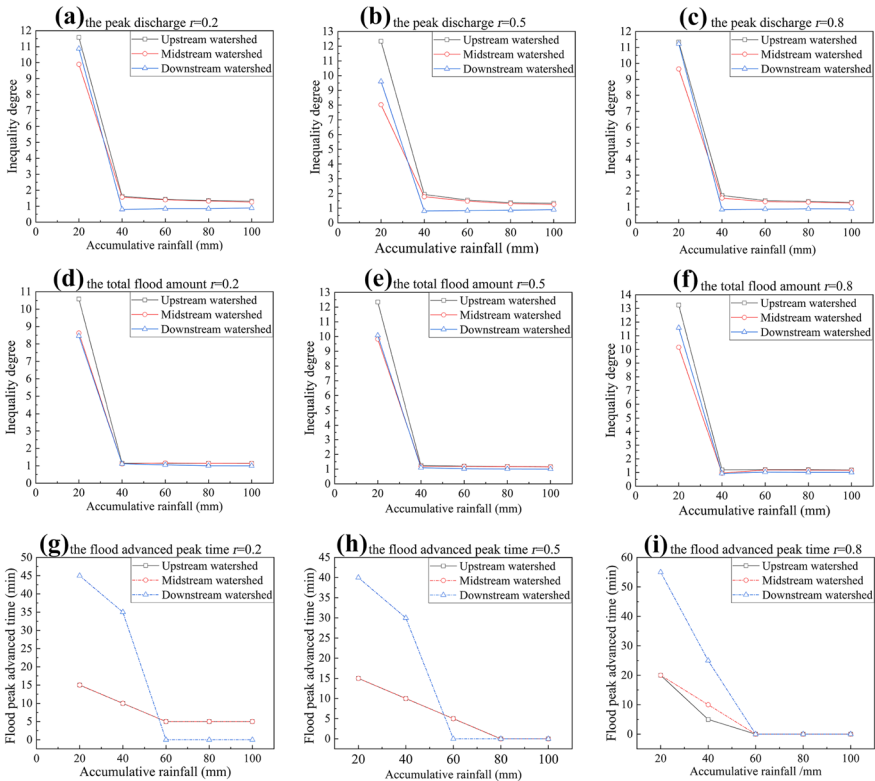


Fig. 6 Variation of discharge characteristics under different rainstorm scenarios

results in moving direction No. 12 is the smallest, and that in moving direction No. 4 is the largest. The average values of different degrees of simulation results in other moving directions are in the range of 0.5~0.8. The lag time of flood peak is provided in Fig. 7b. Compared with the uniform spatial distributed rainstorm, the impact of mobile rainstorm in each moving direction on the flood peak time is basically delayed, and the delay time varies from about 20 min to 180 min. Most of the average delay time is between 50 to 100 min. The inequality degree of flood peak discharge for different accumulative rainfall ($r=0.2$) is illustrated in Fig. 7c. When the rainfall amount increases, the reduction effect of the mobile rainstorm on the flood peak discharge becomes more and more significant. The flood peak discharge can be reduced by up to 30% of the uniform spatial distributed scenario.

4.3 Calculation Equations of Error Correction Coefficient for Flash Flood Discharge Simulation

Based on the simulated data, the rules of the change of discharge characteristics for different spatial-temporal variability of rainstorms are fitted. The calculation equations for different rainstorm characteristics can be obtained. Equations (11)–(13) are the calculation equations for the correction coefficients of the flood peak discharge, the flood peak time

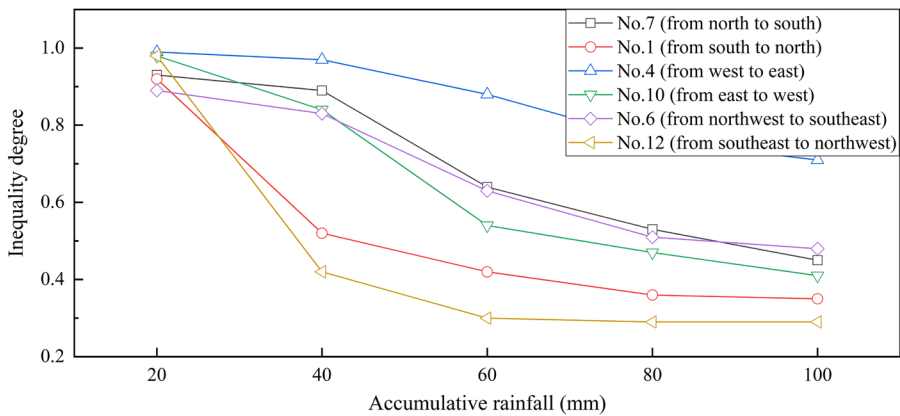
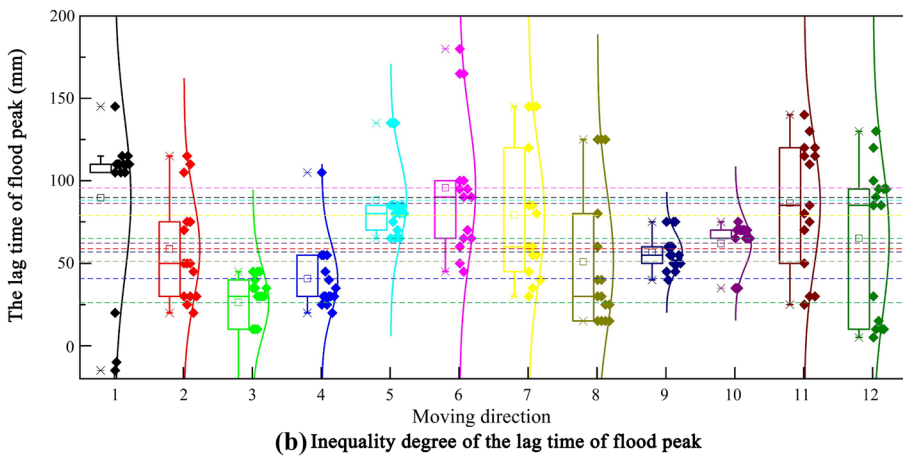
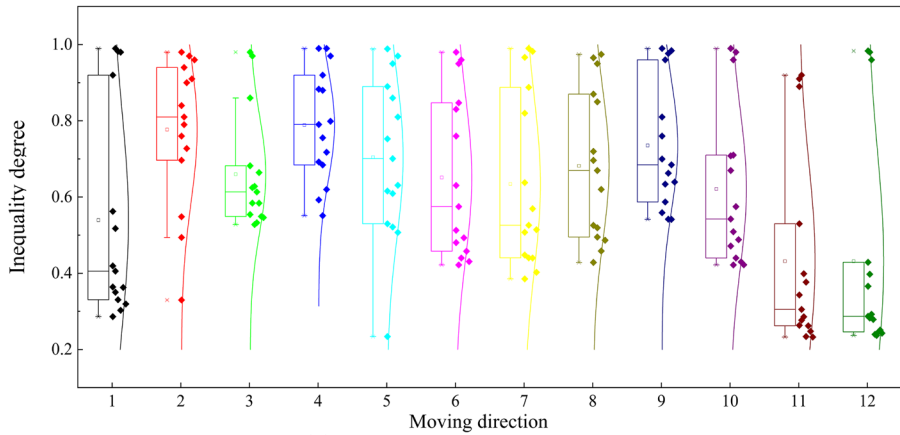


Fig. 7 Inequality degree of discharge characteristics for different rainstorm moving directions

and the total flood volume, respectively, and the correlation coefficient R^2 of these equations all exceed 0.9. If the spatial–temporal variability of rainstorms is not available, single-station rainfall data can be used to simulate the flash flood discharge process. First, the correction coefficients are obtained by inputting the spatial–temporal variability into the formula; then the correction coefficients with the simulated values is multiplied to obtain the corrected data.

$$y_d = \left\{ \left[\begin{matrix} 7.583x_{1,r=0.2}^{-1.309} \\ 6.685x_{2,r=0.2}^{-1.234} \\ 5.832x_{3,r=0.2}^{-1.485} \end{matrix} \right], \left[\begin{matrix} 8.543x_{1,r=0.5}^{-1.360} \\ 6.000x_{2,r=0.5}^{-1.229} \\ 5.310x_{3,r=0.5}^{-1.405} \end{matrix} \right], \left[\begin{matrix} 7.638x_{1,r=0.8}^{-1.317} \\ 6.527x_{2,r=0.8}^{-1.231} \\ 6.100x_{3,r=0.8}^{-1.503} \end{matrix} \right] \right\} \quad (11)$$

$$y_v = \left\{ \left[\begin{matrix} 6.316x_{1,r=0.2}^{-1.324} \\ 5.350x_{2,r=0.2}^{-1.198} \\ 5.380x_{3,r=0.2}^{-1.278} \end{matrix} \right], \left[\begin{matrix} 7.337x_{1,r=0.5}^{-1.407} \\ 6.051x_{2,r=0.5}^{-1.269} \\ 6.100x_{3,r=0.5}^{-1.380} \end{matrix} \right], \left[\begin{matrix} 7.591x_{1,r=0.8}^{-1.422} \\ 5.737x_{2,r=0.8}^{-1.247} \\ 6.413x_{3,r=0.8}^{-1.433} \end{matrix} \right] \right\} \quad (12)$$

$$y_t = \left\{ \left[\begin{matrix} 404.71 \ln(x_{1,2,r=0.2}) - 867.51 \\ 1943.9 \ln(x_{3,r=0.2}) - 2821.3 \end{matrix} \right], \left[\begin{matrix} 605.40 \ln(x_{1,2,r=0.5}) - 939.67 \\ 1717.0 \ln(x_{3,r=0.5}) - 2484.0 \end{matrix} \right], \right. \\ \left. \left[\begin{matrix} 809.42 \ln(x_{1,2,r=0.5}) - 1135.0 \\ 2201.4 \ln(x_{3,r=0.5}) - 3067.8 \end{matrix} \right] \right\} \quad (13)$$

where y_d , y_v and y_t are the correction coefficients of the flood peak discharge, the flood peak time and the total flood volume, respectively; x is the rainfall volume, (mm); subscripts 1, 2 and 3 represent the rainstorm center located in the upstream, midstream and downstream watershed, respectively; subscripts $r=0.2$, 0.5 and 0.8 represent the value of rain peak coefficient.

5 Discussion

5.1 Analysis of the Impact of the Rainstorm Center Location

Topographically, the upstream terrain is the steepest in the entire watershed, it gives the flash flood discharge enormous gravitational potential energy. As a result, when the rainstorm center is at the upstream and midstream watershed, it lengthens the distance of the runoff to the watershed outlet, but the runoff with a high flow velocity has an earlier flood peak time because of the conversion of gravitational potential energy into kinetic energy. From the flow velocity map displayed in Fig. 6b, the gravitational potential energy can speed up flow velocity, and the flooding process turns into a single-peaked pattern, which also increases flood risk. In addition, the time of peak discharge is advanced for this reason. Marchi et al. (2010) pointed out that steepness represents a distinctive morphological feature of flash flood watersheds. Indeed, topographic relief can enhance flash flood occurrence by promoting rapid concentration of runoff.

The inequality degree decreases abruptly when the accumulative rainfall increases from 20 to 40 mm. Because the stable infiltration value of river channel is 20 mm/h, the

infiltration is the major factor affecting the discharge process when the accumulative rainfall is small (20 mm). The rainstorm center at upstream and midstream watershed can speed up the flow velocity, when it is at the downstream watershed it can shorten the flow distance between the runoff and the watershed outlet. Therefore, the time that the runoff stays on the surface is reduced, leading to the significant augment of the flood peak discharge and the total flood volume.

5.2 Analysis of the Impact of Rainstorm Movement Paths

Rainstorm structure, including fine-scale variability and motion, is an important determinant of flood response (Wright et al. 2020). In the case of mobile rainstorm, the rainstorm area does not cover the whole watershed at the beginning, but it expands with time. This kind of rainstorm pattern changes the starting and ending time of runoff in each local region, thus, the runoff from each region in the watershed flow into the river channel at different time. It results in multiple small flood peaks and the flood process becomes flatter. The moving direction No. 6 and No. 12 (rainstorm moving along the river channel) is the farthest distance from all directions. In the moving direction No. 6 and No. 12, the time for rainstorm field extending from the upstream watershed to the watershed outlet is 1.5 h. Due to the inconsistency of rainfall starting and ending time at different rainfall cells, the reduction effect on flood peak is significant, and the average inequality degree of the flood peak discharge is less than 1. Among all moving directions, the rainstorm moves along the river channel from the outlet to the upstream watershed (No. 6), the movement time is the longest, and it maximally separates the runoff process in each rainfall cell, and consequently the flood peak time at the watershed outlet being maximally delayed.

6 Conclusions and Outlook

In this paper, the impact of the spatial–temporal variability of rainstorms on flash flood is investigated by using a hydrodynamic model. The subsequent analysis shows several conclusions:

- (a) When the rainstorm center is at the upstream and midstream watershed, the flash flood with a high flow velocity has an earlier flood peak time and a bigger flood peak discharge because of the conversion of gravitational potential energy into kinetic energy.
- (b) When the rainstorm center is at the upstream and midstream watershed, the total flood volume and the flood peak discharge increase about 2~10 times, and the flood peak time can be advanced by 55 min at most.
- (c) In the mobile rainstorm scenario, the flood peak discharge and the total flood volume are significantly reduced and the flood peak time is lagged; with the increase of accumulative rainfall, the reduced effect of mobile rainstorm on flash flood becomes more obvious. The flood peak discharge can be reduced by up to 30% of the uniform spatial distributed scenario.

There are some deficiencies in this work that need to be supplemented in future studies. This paper focuses on the short-duration and single-peak rainstorm, but does not research the temporal-spatial variability of rainstorms under other conditions, such as bimodal-peak and 24 h long-duration. The flash flood discharge process is jointly

influenced by the temporal-spatial variation of rainstorm, and terrain properties (Wright et al. 2014). This work uses a small watershed terrain, which does not form a river network structure. In further research, more high-resolution rainstorm data with rainstorm structure can be generated by incorporating more characteristic parameters of rainstorm spatial-temporal structure. The study area could be extended in future work with larger watershed scales and complex river network structure by developing a comprehensive analysis framework. Besides, the process of flash flood inundation, including the change of flood level, will also be studied in the future.

Author Contributions Conceptualization and Methodology: J. Hou, G. Chen; Writing-original draft preparation: G. Chen; Material preparation and analysis: S. Yang, Y. Hu, X. Gao; Supervision: T. Wang; Funding acquisition: J. Hou, T. Wang.

Funding This research was supported by the Sino-German Mobility Programme (Grant No. M-0427), the National Natural Science Foundation of China (Grant No. 52079106 and 52009104).

Availability of Data and Materials The data and code that support the study are available from the corresponding author upon reasonable request.

Declarations

Ethical Approval Informed consent.

Consent to Participate Not applicable.

Consent to Publish The authors are indeed informed and agree to publish.

Conflict of Interest We declare that we have no financial and personal relationships with other people or organizations that can inappropriately influence our work, there is no professional or other personal interest of any nature or kind in any product, service and company that could be construed as influencing the position presented in, or the review of, the manuscript entitled “Simulated investigation on the impact of spatial and temporal variability of rainstorms on flash floods in small watershed”.

References

- Ahmadalipour A, Moradkhani H (2019) A data-driven analysis of flash flood hazard, fatalities, and damages over the CONUS during 1996–2017. *J Hydrol (amst)* 578:124106. <https://doi.org/10.1016/j.jhydrol.2019.124106>
- Bubeck P, Thielen AH (2018) What helps people recover from floods? Insights from a survey among flood-affected residents in Germany. *Reg Environ Chang* 18:287–296. <https://doi.org/10.1007/s10113-017-1200-y>
- Ding Z, Qian L, Zhao X, Xia F (2018) Analysis of three echo-trainings of a rainstorm in the South China warm region. *Front Earth Sci* 12:381–396. <https://doi.org/10.1007/s11707-017-0651-2>
- Gires A, Giangola-murzyn A, Abbes J et al (2014) Impacts of small scale rainfall variability in urban areas : a case study with 1D and 1D / 2D hydrological models in a multifractal framework. *Urban Water J* 68:37–41. <https://doi.org/10.1080/1573062X.2014.923917>
- Hou J, Zhang Z, Zhang D et al (2021) Study on the influence of infiltration on flood propagation with different peak shape coefficients and duration. *Water Policy* 23:1059–1074. <https://doi.org/10.2166/wp.2021.193>
- Hu Y, Liu H, Liu H et al (2021) Comparative analysis of two hazard rainstorm processes in Hunan affected by the Southwest China vortex. *IOP Conf Ser Earth Environ Sci*. <https://doi.org/10.1088/1755-1315/865/1/012032>
- Karbasi M, Shokoohi A, Saghafian B (2018) Loss of life estimation due to flash floods in residential areas using a regional model. *Water Resour Manag* 32:4575–4589. <https://doi.org/10.1007/s11269-018-2071-9>
- Keifer CJ, Chu HH (1957) Synthetic storm pattern for drainage design. *J Hydraul Div* 83(4):1–1332. <https://doi.org/10.1061/JYCEAJ.0000104>
- Li H, Hu Y, Zhou Z et al (2018a) Characteristic features of the evolution of a meiyu frontal rainstorm with doppler radar data assimilation. *Adv Meteorol*. <https://doi.org/10.1155/2018/9802360>

- Li J, Deng C, Li H et al (2018b) Hydrological environmental responses of LID and approach for rainfall pattern selection in precipitation data-lacked region. *Water Resour Manag* 32:3271–3284. <https://doi.org/10.1007/s11269-018-1990-9>
- Liang J (2010) Evaluation of runoff response to moving rainstorms. Thesis, Marquette University Wisconsin, USA
- Llasat MC, Marcos R, Llasat-Botija M et al (2014) Flash flood evolution in North-Western Mediterranean. *Atmos Res* 149:230–243. <https://doi.org/10.1016/j.atmosres.2014.05.024>
- Lopez-cantu T, Samaras C (2018) Temporal and spatial evaluation of stormwater engineering standards reveals risks and priorities across the United States OPEN ACCESS Temporal and spatial evaluation of stormwater engineering standards reveals risks and priorities across the United States. *Environ Res Lett* 13:074006. <https://doi.org/10.1088/1748-9326/aac696>
- Marchi L, Borga M, Preciso E, Gaume E (2010) Characterisation of selected extreme flash floods in Europe and implications for flood risk management. *J Hydrol (amst)* 394:118–133. <https://doi.org/10.1016/j.jhydrol.2010.07.017>
- Notaro V, Fontanazza CM, Freni G, Puleo V (2013) Impact of rainfall data resolution in time and space on the urban flooding evaluation. *Water Sci Technol* 68:1984–1993. <https://doi.org/10.2166/wst.2013.435>
- Ochoa-Rodriguez S, Wang LP, Gires A et al (2015) Impact of spatial and temporal resolution of rainfall inputs on urban hydrodynamic modelling outputs: A multi-catchment investigation. *J Hydrol (amst)* 531:389–407. <https://doi.org/10.1016/j.jhydrol.2015.05.035>
- Saharia M, Kirstetter P, Vergara H (2021) On the impact of rainfall spatial variability, geomorphology, and climatology on flash floods. *Water Resour Res* 1–18. <https://doi.org/10.1029/2020WR029124>
- Silvestro F, Rebora N, Giannoni F et al (2016) The flash flood of the Bisagno Creek on 9th October 2014: An “unfortunate” combination of spatial and temporal scales. *J Hydrol (amst)* 541:50–62. <https://doi.org/10.1016/j.jhydrol.2015.08.004>
- Tarolli P, Borga M, Morin E, Delrieu G (2012) Analysis of flash flood regimes in the North-Western and South-Eastern Mediterranean regions. *Nat Hazards Earth Syst Sci* 12:1255–1265. <https://doi.org/10.5194/nhess-12-1255-2012>
- Wright DB, Smith JA, Baeck ML (2014) Flood frequency analysis using radar rainfall fields and stochastic storm transposition. *Water Resour Res* 50:1592–1615. <https://doi.org/10.1002/2013WR014224>
- Wright DB, Yu G, England JF (2020) Six decades of rainfall and flood frequency analysis using stochastic storm transposition: Review, progress, and prospects. *J Hydrol (amst)* 585:124816. <https://doi.org/10.1016/j.jhydrol.2020.124816>
- Yang L, Smith JA, Baeck ML, Zhang Y (2016) Flash flooding in small urban watersheds: Storm event hydrologic response. *Water Resour Res* 52:4571–4589. <https://doi.org/10.1002/2015WR018326>
- Yu Z, Ji C, Xu J et al (2015) Numerical simulation and analysis of the Yangtze River Delta Rainstorm on 8 October 2013 caused by binary typhoons. *Atmos Res* 166:33–48. <https://doi.org/10.1016/j.atmosres.2015.06.014>
- Yuan W, Lu L, Song H et al (2022) Study on the early warning for flash flood based on random rainfall pattern. *Water Resour Manag* 36:1587–1609. <https://doi.org/10.1007/s11269-022-03106-3>
- Yuan W, Tu X, Su C et al (2021) Research on the critical rainfall of flash floods in small watersheds based on the design of characteristic rainfall patterns. *Water Resour Manag* 35:3297–3319. <https://doi.org/10.1007/s11269-021-02893-5>
- Zhang X, Chen J, Lai Z et al (2017) Analysis of special strong wind and severe rainstorm caused by typhoon rammasun in Guangxi, China. *J Geosci Environ Protect* 05:235–251. <https://doi.org/10.4236/gep.2017.58019>
- Zoccatelli D, Borga M, Viglione A et al (2011) Spatial moments of catchment rainfall : rainfall spatial organisation, basin morphology, and flood response. 3767–3783. <https://doi.org/10.5194/nhess-15-3767-2011>
- Zoccatelli D, Borga M, Zanon F et al (2010) Which rainfall spatial information for flash flood response modelling ? A numerical investigation based on data from the Carpathian range, Romania. *J Hydrol (amst)* 394:148–161. <https://doi.org/10.1016/j.jhydrol.2010.07.019>

Publisher's Note Springer Nature remains neutral with regard to jurisdictional claims in published maps and institutional affiliations.

Springer Nature or its licensor (e.g. a society or other partner) holds exclusive rights to this article under a publishing agreement with the author(s) or other rightsholder(s); author self-archiving of the accepted manuscript version of this article is solely governed by the terms of such publishing agreement and applicable law.